Verification of a Varying Threshold Edge Detection SPECT Technique for Spleen Volume: A Comparison with Computed Tomography Volumes

P. Hendrik Pretorius, Andries van Aswegen, Mattheus G. Lötter, Charles P. Herbst, Mariana G. Nel and Anton C. Otto

Biophysics and Nuclear Medicine Departments, University of the Orange Free State, Bloemfontein, South Africa

SPECT enables quantitation of organ volume with radionuclide techniques using threshold edge detection methods. Previous phantom studies showed that a negative correlation exists between volume and threshold value. In those studies, the use of calibration curves were believed to correct for volume dependence on threshold values. The aim of this study was to evaluate the accuracy of spleen volume determination in 20 patients with SPECT by employing a varying threshold edge detection technique with volumes derived from CT. All patients had both radionuclide and CT examinations that were reconstructed with a filtered backprojection algorithm. During SPECT reconstruction, transverse slices were obtained with attenuation correction (Method A) and without attenuation correction (Method B). CT volumes were calculated from manually drawn regions of interest, whereas SPECT volumes were calculated with an automated algorithm using previously determined calibration curves. A confidence interval for calculated SPECT volumes also was calculated because of possible errors in the threshold value. The spleen volumes studied ranged from 91.2 ml to 1660.1 ml. Regression analysis yielded equations of CT = 0.97 SPECT + 7.07 (r = 0.996) and CT = 1.05 SPECT − 19.25 (r = 0.990) between CT and SPECT spleen volumes with a standard error of the y estimates of 31.10 ml and 54.47 ml, respectively. A mean percentage difference of 10.5% ± 7.6% and 11.4% ± 6.6% in spleen volume was obtained for Methods A and B in comparison with CT spleen volumes. The threshold value varied between 40.9% and 32.4% for Method A and between 41.2% and 28.5% for Method B because the spleen volume is increased. The varying threshold edge detection technique described in this paper can be implemented successfully in the clinical setting.

J Nucl Med 1993; 34:963–967

Single-photon emission computed tomography (SPECT) allows the quantitation of organ volume with radionuclide techniques. Edge detection techniques with constant threshold values have been widely used in the calculation of volumes of different organs (*1–9*). Different threshold values, varying from 25% to 51% have been reported, with a value of 43% being used most often (*1–7*). Kavanagh et al. suggested different threshold values to calculate liver and spleen volumes (*1*). In addition to using spleen volume calculations with SPECT in comparative studies with computed tomography (CT) (*1,10*), they were also used to calculate radiation dose to organs (*2,3*), to study optimum processing protocols (*9*) and to study the influence of organ uptake of radionuclides (*10*).

In phantom studies, we showed that a negative correlation existed between organ volume and threshold value (*11*). In that study, different scatter and attenuation correction techniques substantially changed correlation values. We found that the correct threshold value is dependent on the volume under investigation as well as pre-processing (attenuation and/or scatter correction) of the data. Scatter correction was done in accordance with the method proposed by Jaszczak et al. (*12*) and attenuation correction in accordance with Sorenson (*13*). Moreover, these two correction methods were combined. Data then were analyzed without any correction for scatter and attenuation. In each case, the correlation between the threshold value and actual volume could be approximated by a double exponential function with different regression constants, which lead us to suggest the use of these fitted curves for volume measurements using the regression constants obtained from the specific method of acquiring the data and the correction method used.

It is necessary to verify results of a new technique with that of a technique of superior accuracy (*1,10*). Measurement of spleen volume by CT correlates well with anatomical volumes (*14–17*), although there is a possibility of errors being introduced by movement due to respiration (*14,17*).

Received Sept. 11, 1992; revision accepted Feb. 8, 1993.

For correspondence or reprints contact: P.H. Pretorius, Department of Biophysics, University of the Orange Free State, P.O. Box 339, Bloemfontein 9300, South Africa.

The aim of this study was to evaluate the accuracy of measuring spleen volume with SPECT using the varying threshold value method. Spleen volumes obtained from the SPECT study were then compared with those obtained from CT examinations of the abdomen.

METHODS

Patient Group

Twenty consecutive patients ranging in age from 18 to 67 yr (mean: 43 yr) who were referred for a CT study of the abdomen were included. Verbal consent was obtained from all patients for participation in the study. Patients were excluded only when they were too ill to participate or unable to lie still for the duration of the SPECT study.

Data Acquisition and Analysis

SPECT. A General Electric 400 AT Starcam (Milwaukee, WI) scintillation camera fitted with a high-resolution, low-energy, parallel-hole collimator was used for all measurements. Data were acquired through 360° as 64 images in a 128 × 128 matrix format for 20 sec per image 10 min after the administration of 111–185 MBq (3–5 mCi) ^{99m}Tc-labeled tin colloid. The data were reconstructed with a filtered backprojection reconstruction algorithm using a fourth order Butterworth filter and a cutoff frequency of 0.625 cycles/cm (*11*). To determine how accurate volumes could be calculated with different double exponential calibration curves, two methods were investigated. Two sets of reconstructed images were obtained for this purpose, one applying attenuation correction using an attenuation coefficient of 0.012 mm^{-1} (Method A) and the other without any correction for attenuation (Method B). Transverse slices of 1 pixel thickness were obtained for the estimation of spleen volume.

All slices from the reconstructed data set were summed and a region of interest (ROI) was drawn around the spleen using the summed image. Care was taken to exclude all liver activity. The maximum count in the ROI was determined for the summed slices. An initial threshold value of 35% of this maximum count was used to determine which pixels were included within the spleen for each slice. The initial calculated spleen volume was then used to calculate a new threshold value (T_{new}) according to a double exponential function of the form:

$$T_{new} = Ae^{-BX} + Ce^{DX},$$

where X is the volume and A–D are predetermined constants from phantom studies. The process was then repeated until the percentage difference between two consecutive volume calculations was zero. Because of the finite size of the voxels, a zero change in threshold value was obtained within four iterations.

Although the corresponding threshold value can be obtained for a specific volume in this way, previous phantom studies indicated that an uncertainty exists in determining the threshold value for known volumes (*11,18*). By using the double exponential regression curves of the volume/upper and volume/lower values of the threshold confidence limits (*19*), the corresponding uncertainty of the patient threshold value could be determined. These values were then used to calculate the uncertainty in spleen volume.

Computed Tomography. A General Electric 9800 CT scanner was used. Patients were supine and projections were obtained at 360° during maintained inspiration. The data were reconstructed with a filtered backprojection reconstruction algorithm to yield 10-mm thick transverse slices in 512 × 512 matrices. Regions of interest were drawn manually to identify the spleen on each appropriate slice. The area of each ROI was calculated and multiplied by the slice thickness to obtain the spleen volume in each slice. All slices were subsequently summed to determine the total spleen volume.

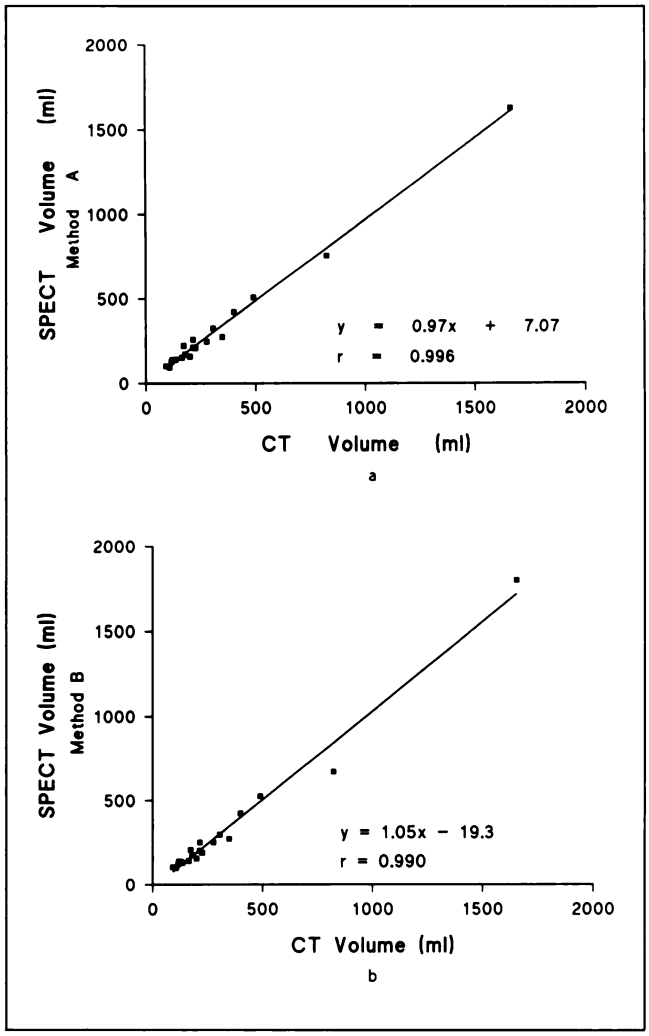

FIGURE 1. Correlation between CT and SPECT volumes obtained with Method A (correction for attenuation) (a) and (b) Method B (no correction).

Statistical Analysis

Linear regression analysis (*19*) as well as intraclass correlations (*20*) were done to compare the spleen volumes obtained from the two SPECT methods with the CT spleen volumes. The value of the difference between the CT and SPECT methods and the percentage difference were also calculated.

RESULTS

Figure 1 shows the regression analysis between the two SPECT methods and CT. Good correlation was obtained between CT and SPECT volumes with regression coefficients of 0.996 for Method A (Fig. 1a) and 0.990 for Method B (Fig. 1b). The standard errors of the y estimate were 31.10 ml and 54.47 ml for the two SPECT methods, whereas the standard errors of the x coefficient were 0.020

TABLE 1
CT and SPECT Volumes with the Confidence Interval for SPECT Volumes

Patient no.	CT (ml)	SPECT Method A (ml)	SPECT Method B (ml)
1	200.3	159.0 (154.6–163.6)	155.1 (151.1–159.1)
2	163.7	152.4 (147.4–157.4)	140.9 (136.2–145.6)
3	225.3	209.6 (202.0–217.2)	189.2 (181.6–197.8)
4	400.3	423.1 (408.0–438.2)	423.6 (408.1–439.1)
5	171.8	222.8 (216.5–229.1)	206.3 (201.7–211.0)
6	305.7	325.3 (310.2–340.8)	297.1 (282.4–311.8)
7	489.6	508.4 (484.9–531.9)	525.4 (497.0–553.8)
8	136.0	141.5 (138.2–144.8)	130.1 (127.2–133.0)
9	91.2	101.9 (99.2–104.6)	103.5 (100.5–106.5)
10	129.0	139.8 (135.6–144.0)	136.4 (132.7–140.1)
11	823.4	757.8 (721.0–794.6)	670.1 (625.0–715.2)
12	118.8	139.0 (134.8–143.2)	139.0 (134.7–143.3)
13	115.7	127.2 (124.1–130.3)	124.3 (121.4–127.2)
14	276.9	246.4 (233.1–259.7)	250.7 (235.1–266.3)
15	214.7	258.4 (245.0–271.8)	251.5 (236.8–266.2)
16	347.8	273.8 (263.0–284.6)	271.8 (263.4–280.2)
17	178.6	172.1 (167.9–176.3)	174.9 (170.8–179.0)
18	106.3	93.9 (90.0–96.4)	97.9 (94.9–100.9)
19	213.9	212.4 (206.4–218.4)	201.4 (195.8–207.0)
20	1660.1	1628.6 (1504.2–1753)	1802.1 (1625.5–1978.7)

and 0.035 respectively. Intraclass correlations gave the same results (1.000 and 0.990 for Methods A and B, respectively) and indicated good agreement between CT measured spleen volumes and spleen volumes obtained with the respective SPECT methods. The volumes obtained from the CT and the SPECT methods, including the confidence interval of the SPECT methods are listed in Table 1. The confidence interval increased with increasing volume. Figure 2 shows threshold value variations with volume obtained with the SPECT methods. The threshold value varied between 40.9% and 32.4% for Method A and between 41.2% and 28.5% for Method B as the volume increased. Table 2 shows the values of the difference and percentage difference between the CT and the two SPECT methods. Maximum differences of 74 ml (Patient 16) with Method A and 153 ml (Patient 11) with Method B were obtained. The mean values for these indices were −3.8 ± 32.7 ml and −3.9 ± 55.8 ml for the two methods, respec-

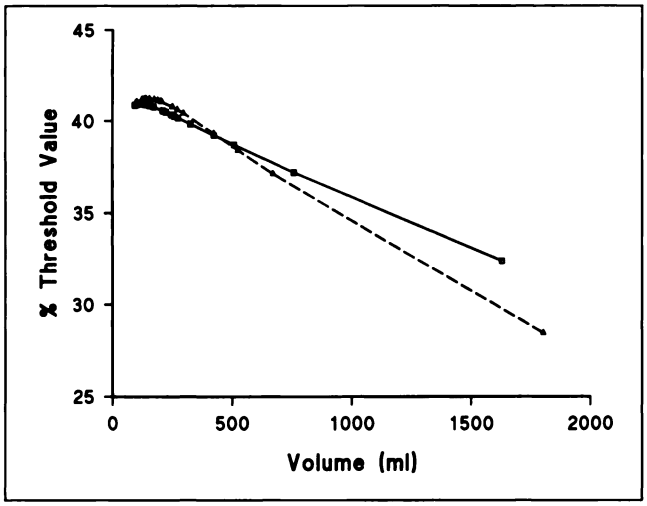

FIGURE 2. SPECT threshold values obtained with (squares) and without (triangles) attenuation correction.

TABLE 2
Values of the Difference and Percentage Difference Obtained Between CT and SPECT Volumes

Patient no.	Method A difference (ml)	Method A difference (%)	Method B difference (ml)	Method B difference (%)
1	−41.3	(20.6)	−45.2	(22.6)
2	−11.3	(6.9)	−22.8	(13.3)
3	−15.7	(7.0)	−36.1	(16.0)
4	22.8	(5.7)	23.3	(5.8)
5	−51.0	(29.7)	−34.5	(20.1)
6	19.6	(6.4)	−8.6	(2.8)
7	18.8	(3.8)	35.8	(7.3)
8	5.5	(4.0)	−5.9	(4.3)
9	10.7	(11.7)	12.3	(13.5)
10	10.8	(8.4)	7.4	(5.7)
11	−65.6	(8.0)	−153.3	(18.6)
12	20.2	(17.0)	20.2	(17.0)
13	11.5	(10.0)	8.6	(7.4)
14	−30.5	(11.0)	−26.2	(9.5)
15	43.7	(20.4)	36.8	(17.1)
16	−74.0	(21.3)	−76.0	(21.9)
17	−6.5	(3.6)	−3.7	(2.1)
18	−12.4	(11.7)	−8.4	(7.9)
19	−1.5	(0.7)	−12.5	(5.8)
20	−31.5	(1.9)	142.0	(8.6)
Mean	−3.8	10.5	−3.9	11.4
s.d.	32.7	7.6	55.8	6.6

tively. The mean values of the percentage difference were 10.5% ± 7.6% and 11.4% ± 6.6% for Methods A and B respectively.

DISCUSSION

A good correlation was found between the measured spleen volumes using CT and SPECT. This finding corresponds with similar studies (*1,10*). It could be argued that larger spleen volumes act as outliers and dominate the regression values (for example, the slope and regression coefficients). If the largest spleen volume is eliminated, the slope for Method B changes by 20%, whereas the regression coefficient changes to 0.972. These indices changed to a lesser extent for Method A (slope = 5.2%, r = 0.983). If the two largest spleen volumes are eliminated, the corresponding changes are less evident and a maximum change of 5.7% occured in the slope of Method B. The intraclass correlations were similar when the same methodology was followed. We believe that the reason for these changes is due to the lack of patients with larger spleen volumes rather than nonlinearity in the method of volume measurement.

The reason for the large deviation in the difference and percentage difference could be attributed to a possible error in CT volume determination. CT data were obtained with patients maintaining inspiration, which could influence the reproducibility of transverse slices during the acquisition of projection data (*14,17*). Another cause of error in CT volumes might be the partial volume effect. In transaxial slices of 10-mm thickness, the partial volume effect could play an important role in the accuracy of slice volume, especially on the periphery of the spleen.

The shape of the spleen volume curve against the threshold value (Fig. 2) confirms our previous finding in phantom studies of an inverse relationship between volume and threshold value (*11,18*). A simulation study reported by King et al. (*21*), however, showed a decrease in threshold value as the ratio of source width (diameter) to system full width at half maximum approximated a value of 2.0, whereas the threshold value started to rise again for smaller ratio values. In our study, the width of smaller spleen volumes probably lies in the range where this ratio approaches 2.0, which could explain the decrease in threshold value as well as the absence of the suggested increase at even smaller volumes.

It is important to know the uncertainty in SPECT volume measurements and their effect when a clinical decision has to be made. The confidence interval obtained from the calibration curves could also serve as an indication of reproducibility for determining threshold values. This value is influenced by positioning, radius of rotation, patient thickness and the partial volume effect.

When regression coefficients and differences between the two SPECT methods were compared, it is clear that implementation of the fitted curves in an automated volume calculation algorithm is a practical solution to determine varying threshold values and spleen volumes. Although the volumes calculated with the two SPECT methods were similar, Method A is favored and implemented in our clinic since higher reconstructed counts are obtained in the transverse slices of the spleen when the uptake of the radionuclide is suboptimal. Furthermore, the regression parameters of Method A are also less dependent on the larger volumes, which is an indication of this method's superiority.

This study showed that a varying threshold edge detection technique can be successfully implemented clinically. On the other hand, we also showed limitations on the method's accuracy and possibly on threshold methods in general. The implementation of such a method by other institutions should be preceded by a calibration phantom study for the scintillation camera, acquisition parameters and correction methods used during analysis.

ACKNOWLEDGMENTS

This work was supported by the South African Medical Research Council and the Central Research Fund of the University of the Orange Free State. The authors thank the Department of Diagnostic Radiology and especially Caren Potgieter for performing the CT scans.

REFERENCES

1. Kavanagh GJ, Kavanagh JT, Kavanagh PBK, Irwin LE, Perkins AC, Swanson LA. Automated volume determination of the liver and spleen from Tc-99m colloid SPECT imaging: quantification of the liver functional and nonfunctional tissue in disease. *Clin Nucl Med* 1990;15:495–500.
2. Iosilevsky G, Israel O, Frenkel A, et al. A practical SPECT technique for quantitation of drug delivery to human tumors and organ absorbed dose. *Semin Nucl Med* 1989;19:33–46.
3. Israel O, Iosilevsky G, Front D, et al. SPECT quantitation of iodine-131 concentration in phantoms and human tumors. *J Nucl Med* 1990;31:1945–1949.
4. Front D, Iosilevsky G, Frenkel A, et al. In vivo quantitation using SPECT of radiopharmaceutical uptake by human meningiomas. *Radiology* 1987; 164:93–96.
5. Tauxe WN, Soussaline F, Todd-Pokropek A, et al. Determination of organ volume by single-photon emission tomography. *J Nucl Med* 1982;23:984–987.
6. Tauxe WN, Todd-Pokropek A, Soussaline F, Raynaud C, Kellershohn C. Estimates of kidney volume by single photon emission tomography: a preliminary report. *Eur J Nucl Med* 1983;8:72–74.
7. Israel O, Front D, Hardoff R, Ish-Shalom S, Jerushalmi J, Kolodny GM. In vivo SPECT quantitation of bone metabolism in hyperparathyroidism and thyrotoxicosis. *J Nucl Med* 1991;32:1157–1161.
8. Faurous P, Saint-Aubert B, Szawlowski A, et al. Estimation of hepatic volume by SPECT during liver regeneration: an experimental study in an animal model. *Nucl Med Biol* 1989;16:375–379.
9. Mut F, Glickman S, Marciano D, Hawkins RA. Optimum processing protocols for volume determination of the liver and spleen from SPECT imaging with technetium-99m sulfur colloid. *J Nucl Med* 1988;29:1768–1775.
10. Strauss LG, Clorius JH, Frank T, Van Kaick G. Single photon emission computerized tomography (SPECT) for estimates of liver and spleen volume. *J Nucl Med* 1984;25:81–85.
11. Pretorius PH, Van Aswegen A, Herbst CP, Lötter MG. The effects of different correction techniques on absolute volume determination with SPECT using a threshold edge detection method. *Med Phys* 1991;18:390–393.
12. Jaszczak RJ, Greer KL, Floyd CE, Harris CC, Coleman RE. Improved SPECT quantification using compensation for scattered photons. *J Nucl Med* 1984;25:893–900.
13. Sorenson JA. Quantitative measurements of radioactivity. In: Hine GJ, Sorenson JA, eds. *Instrumentation in nuclear medicine, volume 2*. New York: Academic Press; 1974:331–348.

14. Breiman RS, Beck JW, Korobkin M, et al. Volume determinations using computed tomography. *Am J Roentgenol* 1982;138:329–333.
15. Henderson JM, Heymsfield SB, Horowitz J, Kutner MH. Measurement of liver and spleen volume by computed tomography. *Radiology* 1981;141: 525–527.
16. Heymsfield SB, Fulenwider T, Nordlinger B, Barlow R, Sones P, Kutner M. Accurate measurement of liver, kidney and spleen volume and mass by computerized axial tomography. *Ann Intern Med* 1979;90:185–187.
17. Jones KR, Robinson PJ. Organ volume determination by CT scanning: reduction of respiration induced errors by feedback monitoring. *J Comp Assist Tomogr* 1986;10:167–171.
18. Pretorius PH, Van Aswegen A, Herbst CP, Lötter MG. A comparison of the effect of different correction techniques on absolute volume determination with two SPECT imaging systems [Abstract]. *Med Biol Eng Comput* 1991; 29:(suppl 2):1014.
19. Mendenhall W. *Introduction to probability and statistics*. California: Duxbury Press; 1971:227–230.
20. Ebel RL. Estimation of the reliability of ratings. *Psychometrika* 1951;16: 407–424.
21. King MA, Long DT, Brill A. SPECT volume quantitation: influence of spatial resolution, source size and shape and voxel size. *Med Phys* 1991; 18:1016–1024.

(continued from page 952)

SELF-STUDY TEST
Skeletal Nuclear Medicine

ANSWERS *(continued)*

2. Francis MD, Fogelman I. ^{99m}Tc diphosphonate uptake mechanisms on bone. In: Fogelman I, ed. *Bone Scanning in Clinical Practice*. London: Springer-Verlag, 1987:7–17.

Items 5-7: Nonosseous Localization of ^{99m}Tc MDP

Answers: 5, E; 6, B; 7, D

Figure 1 shows accumulation of ^{99m}Tc MDP in an axillary lymph node and extravasation of the radiopharmaceutical about the injection site near the wrist. Incidentally noted are foci of increased activity in multiple right anterior ribs, most likely due to fractures. Increased activity in normal axillary lymph nodes ipsilateral to the site of a partially extravasated injection is a common finding on bone scintigraphy and has been confirmed in animal studies. Occasionally, the lymphatic channels containing the tracer in increased concentration also are seen. The mechanism of "retention" of the tracer in the lymph nodes is not entirely clear, but colloid formation (either in the radiopharmaceutical preparation or subsequently in vivo) does not appear to be a prerequisite. In most cases, no hepatic or splenic uptake is seen. Most likely, the higher concentration of ^{99m}Tc MDP in the larger volume of lymph in the node (relative to surrounding soft tissues) accounts for its scintigraphic visualization.

Figure 2 shows markedly increased, diffuse pulmonary uptake of ^{99m}Tc MDP. The most likely cause of this appearance is metastatic calcification, which occurs in hypercalcemic or hyperphosphatemic states when the solubility product for calcium and phosphate is exceeded, leading to deposition of calcium phosphate salts in the extracellular spaces of various soft tissues. The phenomenon is seen in patients with chronic renal failure, hyperparathyroidism, the milk-alkali syndrome, vitamin D intoxication and with hypercalcemia due to neoplastic involvement of the skeleton (metastases, myeloma). Increased tracer accumulation also may be seen in the heart, stomach and kidneys, as well as in the lungs.

Figure 3 illustrates a discrete focus of ^{99m}Tc MDP accumulation in the right upper quadrant of the abdomen, which is both lateral and anterior to the right kidney and, thus, not due to retained pelvicalyceal activity. The most likely explanation for this finding is tracer uptake in a hepatic metastasis that is undergoing either intra- or extracellular calcification. This type of calcification, which most likely is related to necrosis within the tumor deposit, should be considered a form of dystrophic calcification. Unlike metastatic calcification, which occurs as a result of systemic alterations in calcium and phosphate homeostasis, dystrophic calcifications occur at sites of injury (from many different mechanisms) in soft tissues. The primary tumor most often giving rise to "hot" hepatic metastases is adenocarcinoma (especially mucinous) of the colon, but dystrophic calcification has been seen in the metastatic regions of a wide variety of other neoplasms and also occurs in some hepatomas.

If there were excessive free reduced ^{99m}Tc in a preparation of ^{99m}Tc MDP with formation of colloid, the expected scintigraphic finding would be a generalized increase in hepatic and splenic uptake.

Heterotopic ossification includes localized myositis ossificans, which is usually post-traumatic and occurs adjacent to a long bone, and the new bone formation in the soft tissues, most often about the hips, occurring in association with spinal cord injuries, other neurologic disorders and burns. It also occurs as part of a rare hereditary disorder known as myositis (fibrositis) ossificans progressiva.

References

1. Wallis JW, Fisher S, Wahl RL. ^{99m}Tc-MDP uptake by lymph nodes following tracer infiltration: clinical and laboratory evaluation. *Nucl Med Commun* 1987;8:357–363.
2. Gray HW. Soft tissue uptake of bone agents. In: Fogelman I, ed. *Bone Scanning in Clinical Practice*. London: Springer-Verlag, 1987:211–235.

Items 8-10: Evaluation of Bone Mineral Analyses

Answers: 8, C; 9, B; 10, D

A review of the bone mineral tracing is an important part of the interpretation of bone mineral measurements. Figure 4 shows radiographically evident scoliosis and post-traumatic changes in the lumbar spine, which will make bone mineral results from this site difficult to interpret, even if a more superior region of interest is used (e.g., T12, L1). In such cases it is best not to use the lumbar spine as the site of measurement, and to use the hip, the radius or calcaneus instead.

Figure 5 shows degenerative changes in the facet joints, aortic calcification and wedging of L2 on the radiograph, and inhomogeneous distribution of bone mineral in the bone mineral image. The region of interest for bone mineral measurements should exclude L2.

The findings in Figure 6 best correspond to the description in option D. Generally, 10%–15% of women over 65 years of age have significant degenerative or postoperative changes, or have compression fractures in the standard measuring site. In most of these cases, modification of the standard region of interest becomes necessary or another site has to be selected. The error of the method, with respect to both precision and accuracy, increases when the region of interest is smaller. The smallest region of interest used probably should not be less than two vertebrae or about ten scanning lines. Dual-photon absorptiometry detects osteopenia but does not distinguish the multiple causes of decreased bone mineral density from each other.

For further in-depth information, refer to the syllabus pages in Nuclear Medicine Self-Study I.